MOLECULAR AND CELLULAR BIOLOGY, June 2007, p. 4465–4474 Vol. 27, No. 12
0270-7306/07/$08.00+0 doi:10.1128/MCB.00104-07
Copyright © 2007, American Society for Microbiology. All Rights Reserved.

Osteoblast Autonomous P_i Regulation via Pit1 Plays a Role in Bone Mineralization[▽]

Yuji Yoshiko,[1,2]* G. Antonio Candeliere,[2] Norihiko Maeda,[1] and Jane E. Aubin[2]*

Department of Oral Growth and Developmental Biology, Hiroshima University Graduate School of Biomedical Sciences, 1-2-3 Kasumi, Minami-ku, Hiroshima 734-8553, Japan,[1] and Department of Molecular and Medical Genetics, Faculty of Medicine, University of Toronto, 1 King's College Circle, Toronto, Ontario M5S 1A8, Canada[2]

Received 17 January 2007/Returned for modification 1 March 2007/Accepted 5 April 2007

The complex pathogenesis of mineralization defects seen in inherited and/or acquired hypophosphatemic disorders suggests that local inorganic phosphate (P_i) regulation by osteoblasts may be a rate-limiting step in physiological bone mineralization. To test whether an osteoblast autonomous phosphate regulatory system regulates mineralization, we manipulated well-established in vivo and in vitro models to study mineralization stages separately from cellular proliferation/differentiation stages of osteogenesis. Foscarnet, an inhibitor of NaP_i transport, blocked mineralization of osteoid formation in osteoblast cultures and local mineralization after injection over the calvariae of newborn rats. Mineralization was also down- and upregulated, respectively, with under- and overexpression of the type III NaP_i transporter Pit1 in osteoblast cultures. Among molecules expressed in osteoblasts and known to be related to P_i handling, stanniocalcin 1 was identified as an early response gene after foscarnet treatment; it was also regulated by extracellular P_i, and itself increased Pit1 accumulation in both osteoblast cultures and in vivo. These results provide new insights into the functional role of osteoblast autonomous P_i handling in normal bone mineralization and the abnormalities seen in skeletal tissue in hypophosphatemic disorders.

Multiple dynamic cellular events underlie de novo bone formation. Osteoblasts develop, synthesize, and deposit extracellular (osteoid) matrix comprising collagen and noncollagenous proteins and participate in osteoid mineralization. Although much has been learned about the cellular and molecular regulation of sequential stages in the bone formation process, e.g., cellular proliferation and differentiation, osteoid deposition, and mineralization, from in vitro (2) and in vivo (20) models, much remains obscure, including, for example, the contribution of systemic versus local regulatory controls.

The control of systemic inorganic phosphate (P_i) levels is known to be indispensable for bone formation, especially for osteoid mineralization processes, but the parathyroid hormone (PTH) (decreasing serum P_i levels)-vitamin D (increasing serum P_i levels) axis does not fully explain systemic P_i homeostasis (31). For example, fibroblast growth factor 23 (FGF23) (1) and secreted frizzled-related protein 4 (sFRP-4) (9) were identified and found to display the biological properties of the putative circulating phosphaturic factor "phosphatonin," which may be primarily responsible for a variety of hypophosphatemic disorders. In contrast, osteomalacia/rickets occurs in Hyp and Gy mice (murine homologues of X-linked hypophosphatemia) (18) but not in mice lacking the primary renal sodium-dependent phosphate (NaP_i) transporter, Npt2 (6). Analyses of several Hyp mouse models have also suggested that Hyp osteoblasts may have an intrinsic impairment in mineralization (for example, see reference 13). Moreover, the mineralization defects seen in Fgf23-null mice with hyperphosphatemia (34, 35) and FGF23 transgenic (TG) mice with hypophosphatemia (23) cannot easily be explained solely by aberrant control of systemic P_i homeostasis, even taking into consideration the altered serum biochemistry in these mouse models. Thus, attention has been turning to the role of local P_i handling by osteoblasts in bone mineralization.

Two related type III NaP_i transporters, Pit1/Glvr1 (gibbon ape leukemia virus receptor) and/or Pit2/Ram1 (amphotropic retrovirus receptor), have been found in osteoblastic cell lines (21). Stable transfection with a Pit1 antisense (AS) expression plasmid abrogates differentiation and matrix mineralization in MC3T3-E1 cells treated long term (6 weeks) with BMP2 (36). When intracellular P_i is increased via Pit1 overexpression, immortalized human smooth muscle cells switch from a contractile to an osteogenic phenotype (24). Taken together, the data suggest that the Pit1 NaP_i transporter may play a role in bone formation. However, because P_i participates in multiple cellular events including cellular proliferation and differentiation during osteogenesis, separating a putative direct role in mineralization from other developmental activities is important and of particular interest, considering the mineralization defects in hypophosphatemic disorders. To test the hypothesis that osteoblast-mediated P_i handling is crucial for mineralization, we exploited models in vivo and in vitro to assess local P_i effects on mineralization separately from effects on osteoblast proliferation and differentiation. We show that stringent regulation of P_i handling by osteoblasts through the NaP_i transporter Pit1 is indispensable for bone mineralization and that stanniocalcin 1 (STC1), a mammalian homologue of the Ca/

* Corresponding author. Mailing address for Jane E. Aubin: Department of Molecular and Medical Genetics, Faculty of Medicine, University of Toronto, 1 King's College Circle, Toronto, ON, Canada M5S 1A8. Phone: (416) 978-4220. Fax: (416) 978-3954. E-mail: jane.aubin@utoronto.ca. Mailing address for Yuji Yoshiko: Department of Oral Growth and Developmental Biology, Hiroshima University Graduate School of Biomedical Sciences, 1-2-3 Kasumi, Minami-ku, Hiroshima 734-8553, Japan. Phone and fax: 81-82-257-5620. E-mail: yyuji@hiroshima-u.ac.jp.

▽ Published ahead of print on 16 April 2007.

P_i-regulating fish hormone STC (11), acts as an autocrine/paracrine regulator of this osteoblast autonomous P_i regulatory system.

MATERIALS AND METHODS

Cell culture. Twenty-one-day-old fetal Wistar rat calvaria (RC) cells were isolated by sequential collagenase (type I; Sigma, St. Louis, MO) digestion (8). Cells from the last four of five digestion fractions were grown separately in α-minium essential medium supplemented with 10% fetal calf serum and antibiotics for a day. Cells from the four fractions were then pooled and grown at 5,000 cells/cm^2 in 24-well plates or 35-mm dishes in the same medium supplemented additionally with 50 μg/ml ascorbic acid until osteoblasts differentiated (day ~12). Differentiated cells were digested with collagenase/trypsin, respectively, for 5 min and then osteoid-like nodules were selectively recovered by forceps to obtain osteoblastic cell-rich fractions and reseeded at very high cell densities (>20,000 cells/cm^2; designated osteoblast subcultures). Several days later (3 days to a maximum of 5 days), osteoblast subcultures were further supplemented with ≤10 mM β-glycerophosphate (βGP) for 2 days to induce mineralization. Some osteoblast subcultures were switched to serum-free medium containing 0.1% bovine serum albumin for treatment with agents as indicated in particular experiments. Mouse osteoblastic MC3T3-E1 and human osteosarcoma $SaOS_2$ cell lines were routinely cultured with medium as described above. Cultures were maintained at 37°C in a humidified atmosphere with 5% CO_2, and medium was changed every second or third day.

MTT assay. Differentiated cells enzymatically recovered as described above were seeded into 96-multiwell plates. After P_i loading for 96 h with or without foscarnet (phosphonoformic acid trisodium salt hexahydrate; Sigma), cells were cultured with 0.1% MTT [3(4,5-dimethyl-thiazoyl-2-yl)-2,5-diphenyltetrazolium bromide)] for 4 h. Cells were then dissolved in 2-propanol, including 0.04 N HCl, and subjected to spectrophotometry (with absorbance at 590 nm).

Foscarnet, P_i, and recombinant human STC1 treatment. Foscarnet, a competitive inhibitor of NaP_i transport (5), was used at 10, 30, or 300 mg/kg/day in vivo and 1 mM or less in vitro, as indicated in individual figures and tables. P_i ($NaPO_4$) at 1.0 (regular medium), 2.5, 3.0, 3.5, and 6.0 mM in medium was used. Recombinant human STC1 (rhSTC1) was given to rats and cultures at 15 or less μg/kg/day and 20 ng/ml, respectively. These concentrations/doses were based on previous reports (5, 38, 42) and our preliminary experiments to determine effective dose ranges. Reagents or vehicle (phosphate-buffered saline [PBS]) alone were injected subcutaneously into newborn rats (5 to 8 rats per group) over the calvaria at the sagittal suture (26) once daily for 5 days. Foscarnet, one single time with βGP, and rhSTC1, every day from day 1 or day 2 (for combination treatments with oligonucleotides), were added into cultures in particular experiments. Cycloheximide was used at 2 μg/ml.

Whole-mount skeletons and histology. Whole rat bodies were fixed in 95% ethanol, and skinned specimens were then placed in acetone and stained with alcian blue and alizarin red (22). Calvariae were fixed in 10% neutral buffered formalin or 4% paraformaldehyde in PBS, decalcified in 10% EDTA (pH 7.4), at 4°C and embedded in paraffin. The fixed bones were also embedded in glycol/methacrylate for plastic sections. Sections 3 μm in thickness were stained with hematoxylin and eosin, von Kossa and toluidine blue, toluidine blue alone, or trichrome stain.

Biochemical parameters in serum. A $1,25(OH)_2D$ radioimmunoassay kit (TFB, Tokyo, Japan) was used to measure $1,25(OH)_2D_3$ in serum pooled from 7 rats per group. Serum Ca, P_i, and alkaline phosphate (ALP) were measured by using colorimetric (for Ca and ALP) and UV (for P_i) determination kits (Sigma). All kits were used according to manufacturer's instructions.

AS oligonucleotide treatments. All oligonucleotides (Biosource, Camarillo, CA) had their internucleotidic linkages phosphorothioated at both the 5′ and 3′ ends as described previously (33). Inverted (INV) and scrambled (SCR) sequences were used as controls for AS sequences. The sequences of the AS and SCR oligonucleotides were as follows: STC1 and AS, 5′-TCACTGCTGAGTTTTGGAGCAT-3′, and SCR, 5′-TATGGTCTGTGTCGAACTCTAG-3′; Pit1 and AS, 5′-GGGGCCAGGGTAGATGCCAT-3′, and SCR, 5′-GAGGGTCAATACGTCCGAGGG-3′; Pit2 and AS, 5′-AGATACCCATCCATGGCCAT-3′, and SCR, 5′-TACACGTCTGACAGACCTAC-3′. Oligonucleotides (STC1, 3 μM; Pit1 and Pit2, 2 μM each) were added to osteoblast subcultures every day from day 1 to culture termination (day 5). For combination treatment with pQE plasmids, osteoblast subcultures were treated with oligonucleotides from day 2.

Human Pit1 overexpression. Human Pit1 (hPit1) full-length cDNA in the EcoRV and XhoI cloning sites was prepared from a human cementing fibroma cell line and ligated into pQE-TriSystem (QIAGEN, Hilden, Germany). Osteoblast cultures (day 1) were transfected with 0.5 μg pQE-TriSystem-hPit1 (pQE-hPit1) or an empty plasmid as a control with TransFast transfection reagent (Promega, Madison,WI) and further incubated for 7 days.

Reverse transcription (RT)-PCR and real-time RT-PCR. Total RNA was prepared using TRIzol reagent (Invitrogen, Carlsbad, CA), and cDNA synthesis and PCR amplification were performed using standard protocols (Toyobo, Osaka, Japan, and QIAGEN). Primer sets for rat STC1, ALP, osteopontin (OPN), the type I NaP_i transporter (NPT1), NPT2b, NPT2c, brain-specific NaP_i transporter (BNPI), Pit1, Pit2, and L32 (ribosomal protein L32 as an internal control) were designed using Primer Picking (Primer 3) and were as follows: STC1, 5′-CTGCCTCAACAGTGCCCTAC-3′ and 5′-GGAGGTTCCTGAGGAGGACT-3′; OPN, 5′-AGAGGAGAAGGCGCATTACA-3′ and 5′-GCAACTGGGATGACCTTGAT-3′; NPT1, 5′-AGAGAGAATGGGCTGCTGTC-3′ and 5′-AAGCTTCAGGCTACCGGTCT-3′; NPT2b, 5′-AGAGGGCATATCCACTCACG-3′ and 5′-GTATTGTCAAAGCCCCCAGA-3′; BNPI, 5′-TGAGGATCCTTCAGGGATTG-3′ and 5′-CAGTCCCACCTTGCTGATCT-3′; NPT2c, 5′-AGACTGCTCTGCCATCACCT-3′ and 5′-CAGTCTCAAGACAGGCACCA-3′; Pit1, 5′-TGTGATGTCTTGGTTCGTCT-3′ and 5′-AGGTTGCCATTAGGCAACTG-3′; Pit2, 5′-GACTCCCAATCTCAGGGACA-3′ and 5′-TCCTGAGCTGGTTTCTCCTC-3′; L32, 5′-CATGGCTGCCCTTCGGCCTC-3′ and 5′-CATTCTCTTCGCTGCGTAGCC-3′. Primers for NPT2a (17), described previously, were 5′-TATCATCCAGCTGGACAAGTC-3′ and 5′-CAGGGAGAAGCTCTCCAGCTC-3′. Full-length hPit1 cDNA was obtained using primers 5′-GGCAACGCTGATTACCAGTACTACAGCT-3′ and 5′-GGAACTCGAGTCACATTCTGAGGATGACAT-3′ (the recognition site of XhoI used for cloning is underlined). ReverTraAce (Toyobo) and QIAGEN *Taq* polymerase/ProofStart DNA polymerase (for full-length hPit1) were used for RT and PCR, respectively. PCR was performed for 18 to 38 cycles of 94°C for 30 s, 56°C for 30 s, and 72°C for 30 s (2 min for hPit1). To quantify reaction products, at least four different cycles over the linear phase were chosen for each target. Reaction products were separated by electrophoresis using a 1% agarose gel. Bands were visualized by UV illumination of ethidium bromide-stained gels and captured using an ATTO Densitograph system (Tokyo, Japan). Band intensity was quantitatively analyzed in three independent experiments by Densitograph software (ATTO) for each gene and was normalized to corresponding L32 values. Real-time RT-PCR was also carried out in triplicate by using a LightCycler system (SYBR Green 1; Roche Diagnostics, Indianapolis, IN) according to the manufacturer's instructions. Each product was confirmed by subcloning and sequencing or by the determination of melting curves.

Western blotting. Cells were lysed in RIPA buffer (1% Triton X-100, 1% sodium deoxycholate, 0.1% sodium dodecyl sulfate [SDS], 158 mM NaCl in 10 mM Tris-HCl [pH 7.2], 1 mM EGTA, 100 μg/ml leupeptin, 1 mM phenylmethylsulfonyl fluoride [PMSF], 1 mM Na_3VO_4). Proteins (20 μg) were resolved by SDS-polyacrylamide gel electrophoresis on 15% gels under reducing conditions and electroblotted onto nitrocellulose membranes. The membranes were incubated with TTBS (0.1% Tween 20 and 0.1 M NaCl in 0.1 M Tris-HCl [pH 7.5]) containing 0.2% casein for 2 h and with anti-rhSTC1 monoclonal (0.5 μg/ml) antibody (42), anti-Pit1 and Pit2 antibodies (Alpha Diagnostic International, San Antonio, TX) or anti-His monoclonal antibody (QIAGEN) at 4°C overnight. The membranes were then treated with a horseradish peroxidase-conjugated second antibody (Santa Cruz Biotechnology, Santa Cruz, CA) for 2 h, followed by chemiluminescence detection (Lumi-LightPLUS Western blotting substrate; Roche Diagnostics). Equal loading of proteins was confirmed by anti-actin antibody (Santa Cruz Biotechnology).

ALP von Kossa staining. For histochemical analysis of ALP activity and matrix mineralization, cultures were fixed in neutral buffered formalin at 4°C for 15 min, treated with naphthol AS MX/red violet LB in 0.1 M Tris-HCl (pH 8.3), followed by incubation with 2.5% silver nitrate solution (8).

NaP_i transport assay. Regular RC cell cultures and osteoblast subcultures treated with or without rhSTC1 for 3 days under serum-free conditions were washed with washing buffer (150 mM choline chloride, 1.8 mM $MgCl_2$, 1 mM $CaCl_2$, and 10 mM HEPES buffered with Tris-HCl [pH 7.4]) and NaP_i transport was measured with or without Na^+ in the presence of 0.1 mM KH_2PO_4 (1 μCi/ml $^{32}P_i$; Amersham, Piscataway, NJ) at 37°C. After 10 min, the cells were washed, dried, and solubilized in 0.2 N NaOH. P_i uptake was determined by liquid scintillation counting (39). The raw data (in cpm) were transformed to nmol/mg protein.

Statistical analysis. Data are expressed as means ± standard deviations of replicate samples (n = 3 to 8, depending on the experiment), and experiments were repeated a minimum of two to three times. Statistical significance of differences was evaluated by analysis of variance and post hoc Student's t test.

RESULTS

Osteoid mineralization is controlled by osteoblast-mediated NaP_i transport. We found that NaP_i transport increased and reached a maximum at the mature osteoblast stage in differentiating fetal RC cell cultures (Fig. 1A and B), suggesting that P_i requirements in osteoblasts are larger than those in osteoprogenitor cells. To determine whether local NaP_i transport plays a role in mineralization separate from a role in proliferation-differentiation, we treated mature RC subcultures (cultures in which osteoblasts had already differentiated and matrix was deposited but had not yet mineralized; designated osteoblast subcultures; Fig. 1A) with foscarnet, a selective inhibitor of NaP_i transport (5). Such osteoblast subcultures at very high cell densities reached confluence, expressed mRNAs for osteoblast markers (i.e., Runx2, ALP, OPN, BSP, and OCN), and mineralized their matrix quickly (within a few days) in the presence of βGP without forming nodules; this was in contrast to primary RC cell cultures in which ALP-positive and nodule-forming cells form via a proliferation-differentiation sequence such that discrete foci form over a period of approximately 14 or more days, with resultant increases in ALP, BSP, and OCN mRNA expression (Fig. 1C).

In osteoblast subcultures, foscarnet (≤1 mM) inhibited mineralization (Fig. 1C) with a decrease in NaP_i transport (Fig. 1D) and mRNA for OPN, a marker of osteoblast response to P_i (5), but with no apparent changes in either ALP staining or ALP, BSP, OCN, and Runx2 mRNA levels (Fig. 1C and E). Notably, mineralization was enhanced with a concomitant increase in OPN mRNA when extracellular P_i was increased (Fig. 1F). Low concentrations (≤4 mM) of P_i had no detectable effect on cell viability/activity as judged by morphology and ALP staining or by the MTT viability index (not shown), while P_i overloading (≥5 mM, representative MTT data at 7 mM are shown in Fig. 1G) induced cell death (apoptosis, see reference 25). These effects were abrogated by foscarnet treatment (Fig. 1F and G), suggesting that osteoblasts stringently regulate NaP_i transport for mineralization.

To extend these results to an in vivo bone formation model (26), we injected foscarnet over the calvaria of newborn rats. Preliminary experiments allowed identification of concentrations of foscarnet with no detectable systemic effects: pups given foscarnet at doses of 30 mg/kg/day and lower had normal levels of serum Ca, P_i, ALP, and $1,25(OH)_2D_3$ as well as body weight (Table 1). Thus, we chose 30 mg/kg/day of foscarnet to study further the effects of local blocking of NaP_i transport on calvarial bone formation. In whole-mount skeletons double stained for bone and cartilage, we observed a mineralization defect in calvarial bones but no detectable delay or impairment of mineralization in other parts of the facial, axial, or appendicular skeleton (Fig. 2A to C). Higher magnification views of the parietal bone close to the sagittal suture indicated that toluidine blue-positive unmineralized osteoid matrix comprised narrow seams in the control group but very wide seams in the foscarnet-treated group (Fig. 2D); von Kossa and trichrome staining supported these observations (data not shown). The wide osteoid seams of foscarnet-treated calvariae were covered with cuboidal osteoblasts that were histologically indistinguishable from control osteoblasts (Fig. 2E and F). Other histological features were also similar between foscar-

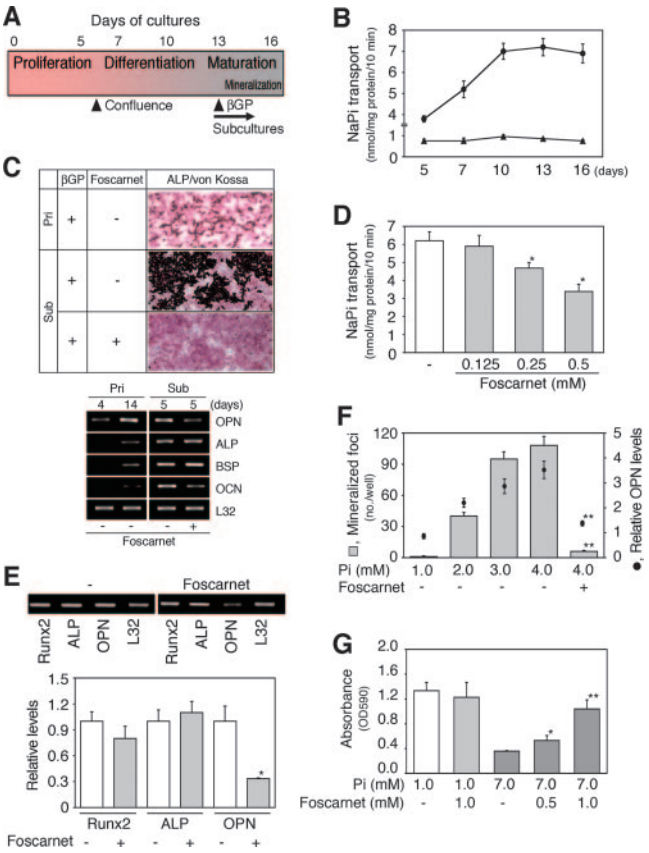

FIG. 1. NaP_i transport is closely correlated with mineralization in vitro. (A) Outline of proliferation-differentiation-maturation sequence in RC cell cultures. Cells actively proliferate, reach confluence (day 6), and subsequently differentiate and mature (day 13). When mature cells at days 13 to 14 were subcultured at a high cell density, mineralization was quickly initiated within 36 h in mature osteoblast cultures when βGP was added. (B) NaP_i transport during osteoblast development in primary differentiating RC cell cultures. NaP_i transport reached a maximum when cells fully differentiated and matured. Round and triangle symbols show P_i transport in the presence and absence, respectively, of sodium. (C) Typical ALP/von Kossa staining (upper panels) and osteoblast marker mRNA levels (lower panels) in primary (Pri) cultures (day 20) and osteoblast subcultures (Sub, day 6 after subculture of day 14 mature osteoblast primary cultures) in the presence of 10 mM βGP and with or without 0.5 mM foscarnet. Osteoblast subcultures uniformly stained with ALP (red) and manifested increased mineralized areas (black) in comparison to that of parallel primary cultures; foscarnet completely inhibited mineralization in osteoblast subcultures. (D) Foscarnet dose dependently inhibits NaP_i transport in osteoblast subcultures. (E) Foscarnet decreases OPN mRNA but not Runx2 and ALP mRNA levels in osteoblast subcultures. Osteoblast subcultures (day 2) were treated with 0.5 mM foscarnet for 2 days in the presence of 5 mM βGP. Semiquantitative RT-PCR data are shown along with a representative agarose gel (upper panels). L32 was used as an internal control. *, $P < 0.05$, compared with vehicle (−). (F) The NaP_i transporter is involved in mineralization. P_i loading to less than 4 mM increased not only mineralization but also OPN mRNA levels (semiquantitative RT-PCR as shown in panel E) in osteoblast subcultures, which was abrogated by treatment with 0.5 mM foscarnet. **, $P < 0.01$, compared with vehicle (−). (G) Overloading of P_i causes cell death via the NaP_i transporter. The MTT assay reveals that foscarnet dose dependently blocked P_i-dependent cell death. Osteoblast subcultures were treated with P_i (7 mM) with or without foscarnet for 4 days. *, $P < 0.05$, and **, $P < 0.01$, compared with matched vehicle control (−).

TABLE 1. Effects of local injections of foscarnet on the newborn rat calvaria for 5 days on serum and body weight parameters

Foscarnet dosage (mg/kg/day)	Effects of foscarnet injection (± SD) on the indicated parameters[a]					
	Body wt (g)		Serum concn			
	Day 0	Day 4	Ca (mg/dl)	P_i (mg/dl)	ALP (U/liter)	$1,25(OH)_2D_3$ (pg/ml)
Control	6.36 ± 0.35	12.3 ± 0.35	10.3 ± 0.53	8.7 ± 0.22	242 ± 13	157
10	6.40 ± 0.36	12.9 ± 0.41	10.1 ± 0.37	9.0 ± 0.27	234 ± 12	152
30	6.46 ± 0.32	12.6 ± 0.35	10.1 ± 0.31	8.9 ± 0.23	247 ± 18	163
300	6.46 ± 0.29	10.4 ± 0.70*	8.8 ± 0.43*	7.7 ± 0.42*	ND	ND

[a] Values shown are means ± standard deviations. *, $P < 0.05$, compared with control. ND, not detected.

net-treated and control treatment groups (Fig. 2E and F). Histomorphometry indicated that the osteoblast number and the total bone thickness were not different, but osteoid thickness was greater in foscarnet-treated than vehicle-treated calvariae (Fig. 2G). Thus, blocking NaP_i transport locally in the growing calvariae of newborn rats elicits a regional mineralization defect without changes in systemic P_i homeostasis. Taken together with the NaP_i transport activity and foscarnet effects in vitro (Fig. 1), our data suggest that mineralization is more sensitive to NaP_i transport than other bone formation processes.

The NaP_i transporter Pit1 is required for mineralization in osteoblast subcultures. Among NaP_i transporters identified to date, we found predominantly Pit1 and Pit2 with low amounts of BNPI expressed in RC osteoblast subcultures (Fig. 3A and B) as well as MC3T3-E1 and SaOS2 cells (data not shown). NPT1, NPT2a, and NPT2b were not detected in osteoblastic cells. There was an excellent correlation between the accumulation of Pit1 and Pit2 proteins (detected as a single band about 95 kDa in size, respectively; Fig. 3C) and NaP_i transport activity (Fig. 1B) as osteoblasts differentiated, although their mRNA levels were downregulated. Given this, and the fact that Pit1 activity has been implicated in both smooth muscle (24) and BMP2-treated MC3T3-E1 (36) cell function, we next asked whether one or both Pit proteins are functionally active in mineralization in osteoblast subcultures. Specific knockdown of Pit1 but not Pit2 by AS oligonucleotides inhibited mineralization (Fig. 3D). Pit1 AS oligonucleotides also blocked expression of OPN but not ALP (whose disruption abrogates mineralization in vivo and in vitro (41 and see below) (Fig. 3E). Consistent with these results, mineralization was increased in hPit1-expressing cells (transient transfection with pQE-hPit1) (Fig. 3F). It is also worth noting that overexpression of hPit1 downregulated endogenous Pit1 levels (Fig.

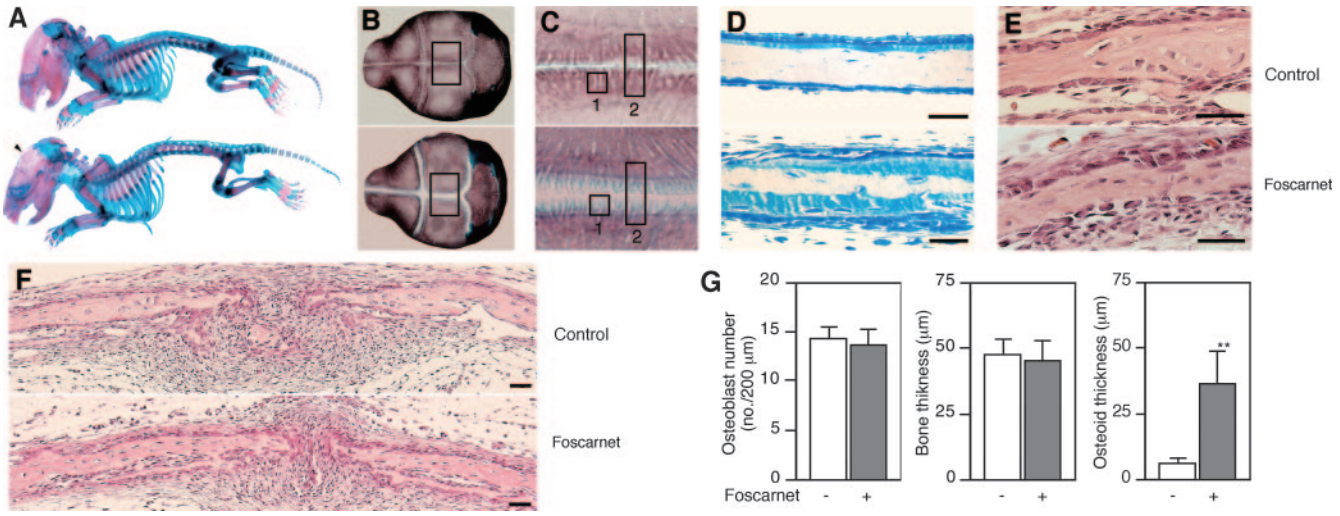

FIG. 2. Foscarnet injections over the sagittal suture of calvariae of newborn rats block mineralization of calvaria but not other skeletal elements. (A to F) Upper and lower panels show the vehicle (control)- and foscarnet-treated groups, respectively. (A to C). Whole-mount skeletons double stained with alcian blue (cartilage) and alizarin red (calcified bone) show that only the calvarium (arrowhead) is affected in rats treated with foscarnet over the calvaria. (A) Whole-body specimens show no systemic effects of locally injected foscarnet on any skeletal elements other than calvaria. (B) Higher magnification of the skulls shown in panel A. (C) Higher magnification of the enclosed areas in panel B. Markedly less mineralization is seen in foscarnet-treated calvariae; note the region stained with alcian blue but not with alizarin red. (D and E) Transverse sections of areas shown in boxes 1 and 2 in panel C. (D) Toluidine blue staining of plastic sections. A wider unmineralized seam (light blue staining) is seen in foscarnet-treated calvariae. (E and F) Hematoxylin and eosin staining of decalcified paraffin sections. No detectable histological differences other than the width of the osteoid seam, as shown in panel D, was seen between the two groups. Scale bars represent 50 μm. (G) Histomorphometric analyses of the osteoblast number (ectocranial surface), the width of the parietal bones, and the osteoid width in foscarnet- versus vehicle-treated bones. Measurements were made between 200 and 600 μm laterally from the sagittal suture. **, $P < 0.01$, compared with vehicle.

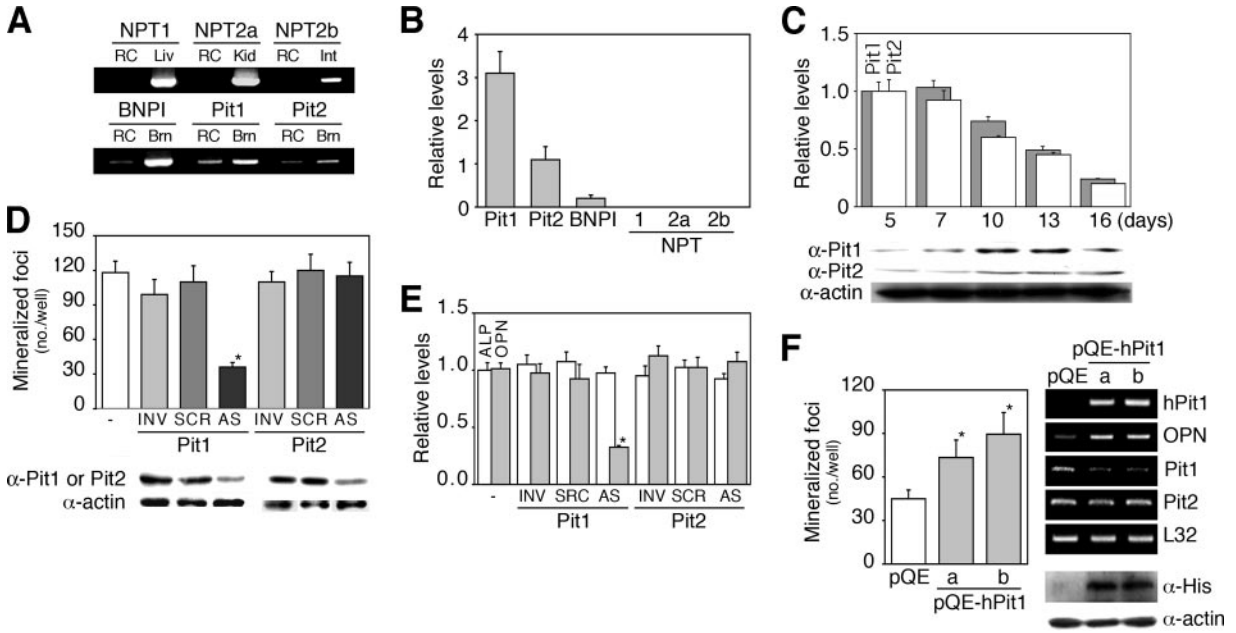

FIG. 3. Pit1, the major type III NaP_i transporter in osteoblasts, is essential for mineralization in vitro. (A) RT-PCR analysis of known NaP_i transporters in RC cells. Pit1, Pit2, and BNPI, but neither NPT1, NPT2a, nor NPT2b, were detected. RC, RC cells (day 13 cultures). Liver (Liv), kidney (Kid), intestine (Int), and brain (Brn) tissues were used as positive controls. RT-PCR data are shown as a representative agarose gel. (B) Relative levels of NPT mRNAs in osteoblast subcultures. Real-time RT-PCR reveals that Pit1 mRNA is most abundantly expressed in osteoblasts, followed by that of Pit2; BNPI is only faintly detected. (C) Pit mRNA expression and protein accumulation during osteoblast development in primary RC cell cultures are shown. Real-time RT-PCR shows a decrease in Pit1 and Pit2 mRNA levels during osteoblast development. In contrast, a representative Western blot reveals a gradual increase in Pit1 and Pit2 proteins as osteoblasts mature (Fig. 1A). (D) AS knockdown of Pit1 but not Pit2 inhibits mineralization. Osteoblast subcultures were untreated or were treated with oligonucleotides (2 μM; AS, antisense; SCR, scrambled; INV, inverted) specific to Pit1 or Pit2 for 5 days. A representative Western blot shows specific effects of Pit1 and Pit2 AS oligonucleotides on their corresponding protein levels. *, $P < 0.05$, compared with vehicle (−). (E) AS knockdown of Pit1 decreases OPN but not ALP mRNA levels in osteoblast subcultures. Semiquantitative RT-PCR was performed with cultures parallel to those used for mineralization studies in panel D. (F) Cells overexpressing hPit1 express the phenotype opposite to those in the AS experiment. *, $P < 0.05$, compared with empty vector (pQE). hPit1 mRNAs in day 3 cultures and Pit1, Pit2, and OPN mRNA levels in day 5 cultures and His-tagged hPit1 in immunoblots at day 3 cultures are shown. Lanes a and b indicate osteoblasts transfected independently with two different pQE-hPit1 plasmids. Osteoblast subcultures were transfected with pQE plasmids at day 1 and further incubated for 5 days. Mineralization effects are shown with a representative agarose gel on the right (upper black lanes, RT-PCR) and Western blot (lower two lanes). L32 and actin were used as internal controls, shown in panels B, E, and F and in panels C, D, and F, respectively.

3F). Together with the cell death seen at high extracellular P_i levels (Fig. 1G), these data demonstrate that specific levels of P_i achieved via the Pit1 NaP_i transporter in osteoblasts are required for mineralization.

STC1 is involved in P_i-mediated mineralization in osteoblast subcultures. To elucidate the regulatory pathway that links an osteoblast-resident P_i-sensing system to matrix mineralization, we performed semiquantitative RT-PCR and screened control versus foscarnet-treated (12 h) osteoblast subcultures for differential expression of a candidate (foscarnet-sensitive early) gene(s) that might regulate NaP_i transport. In addition to FGF23 (1) and sFRP-4 (9), we screened dentin matrix protein 1 (DMP1) (12) and matrix extracellular phosphoglycoprotein (MEPE) (32), which have been isolated from tumors associated with hypophosphatemia. We also assessed a variety of factors expressed in osteoblasts and previously shown to alter NaP_i transport in osteoblastic cell lines, such as PTH-related peptide (PTHrP) (30), transforming growth factors (TGFs) (30, 28), insulin-like growth factor (IGF)-I (29), platelet-derived growth factor (PDGF) (44), and basic fibroblast growth factor (37). In addition, we assessed STC1, a molecule we have shown to upregulate NaP_i transport in differentiating osteoblastic cells (42). Among the molecules screened (Table 2) in cells treated transiently with foscarnet, we found only STC1 mRNA significantly upregulated within 12 h in response to foscarnet, concomitant with upregulation of ALP (~12 h) and followed by sequential increases in Pit1 (~24 h) and Pit2 (~48 h) mRNA levels (Fig. 4A). OPN mRNA expression was initially decreased (~12 h) and then returned to the basal level within 48 h.

To confirm that STC1 expression is sensitive to changes in NaP_i transport and P_i levels, we also determined whether P_i loading (treatment with 10 mM βGP) alters STC1 mRNA expression in osteoblast subcultures. STC1 was downregulated by 48 h after the addition of βGP when the cultures were completely mineralized but not at 24 h when mineralization was in progress (Fig. 4B). We next asked whether STC1 is involved in matrix mineralization independently of its stimulatory effect on osteoblast differentiation seen in primary RC cell cultures (data not shown) (42). To do this, we again used the osteoblast subculture model and found that recombinant human STC1 (rhSTC1) increased NaP_i transport, concomitant with increased mineralization and OPN mRNA levels (Fig. 4C). Because AS knockdown of STC1 elicited a mirror image

TABLE 2. Candidates for a regulatory factor that are expressed in osteoblasts and that link the osteoblast Pit1-P_i system to mineralization[a]

Group	Factor	Reference(s)
P_i-regulating factors isolated in tumor-induced osteomalcia	FGF23	ADHR Consortium (1)
	sFRP 4	Berndt et al. (9)
	DMP-1	De Beur et al. (12)
	MEPE	Rowe et al. (32)
Osteotropic factors	PTHrp	Pizurki et al. (30)
	TGFs	Pizurki et al. (30); Palmer et al. (28)
	IGF-I	Palmer et al. (29)
	PDGF	Zhen et al. (44)
	Basic FGF	Suzuki et al. (37)
	STC1	Yoshiko et al. (42)

[a] Under our treatment protocol conditions, most factors either did not change or changed expression levels <50% in response to foscarnet; STC1 increased expression fourfold.

effect of the recombinant protein and further decreased Pit1 mRNA expression (Fig. 4D), we conclude that STC1 is involved in P_i-mediated mineralization in the osteoblast subculture model.

STC1 functionally contributes to Pit1-mediated mineralization in vitro and in vivo. To address whether STC1 is functionally linked to Pit1-mediated mineralization, we treated osteoblast subcultures with rhSTC1 in combination with Pit1 AS oligonucleotides (Fig. 5A). Notably, rhSTC1 partially rescued cultures from the decreases in NaP_i transport, mineralization, and OPN mRNA expression (Fig. 4C) that resulted from AS knockdown of Pit1. Treatment of osteoblast subcultures for 3 h with rhSTC1 under serum-free conditions increased Pit1 mRNA when cycloheximide was also present, suggesting superinduction (conventionally regarded as a secondary consequence of translational arrest) (14) (Fig. 5B). We also examined the consequence of AS knockdown of STC1 in osteoblast subcultures overexpressing hPit1 by transfection of pQE-hPit1. While AS knockdown of STC1 decreased mineralization concomitantly with lower levels of Pit1 and OPN mRNA (Fig. 4D), it did not reverse the increases seen after transfection of

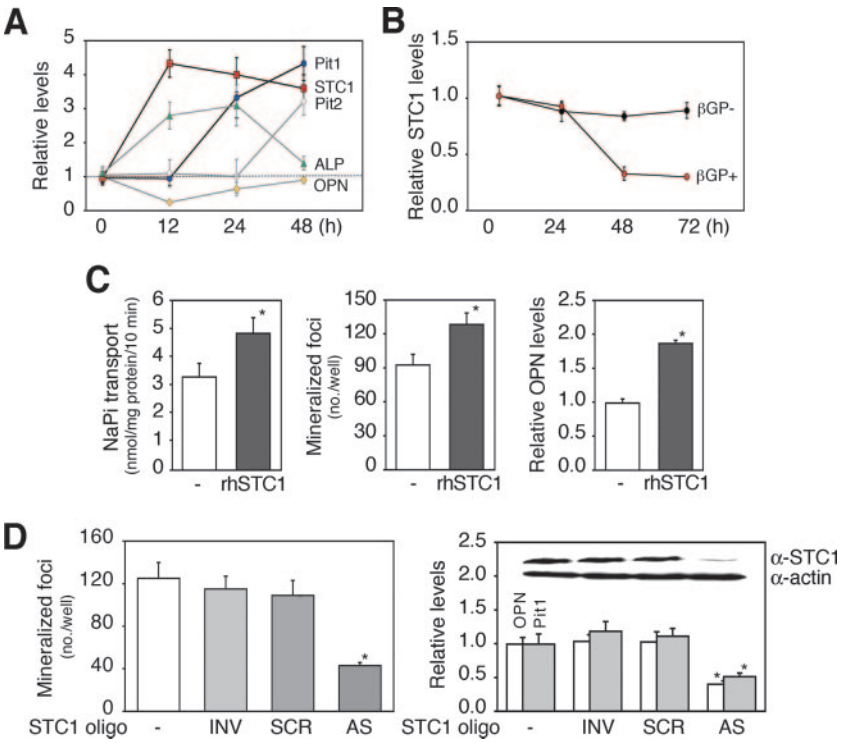

FIG. 4. STC1 is coupled with P_i-mediated mineralization in vitro. (A) Sequential changes in expression levels of OPN, Pit1, STC1, and ALP mRNAs in cells treated with foscarnet. Osteoblast subcultures were treated with 0.5 mM foscarnet for 12 h and then screened for foscarnet-sensitive rapid response genes by semiquantitative RT-PCR. Among molecules screened (Table 2), only STC1 changed significantly (fourfold increase) by 12 h, and this was followed by an increase in Pit1 mRNA levels by 24 h. (B) STC1 mRNA levels were downregulated by βGP. Osteoblast subcultures were treated with 10 mM βGP at the times indicated and then subjected to real-time RT-PCR. STC1 mRNA levels decreased when mineralization was completed (~48 h). (C) rhSTC1 increases NaP_i transport, mineralization, and OPN mRNA expression in osteoblast subcultures. Cultures were grown under the same conditions as described for panel B; cultures were treated with 20 ng/ml rhSTC1 for 3 days under serum free-conditions for the NaP_i transport assay and for 5 days under normal conditions for mineralization and OPN mRNA expression (semiquantitative RT-PCR). *, $P < 0.05$, compared with vehicle (−). (D) Cells with AS knockdown of STC1 expressed the opposite phenotypes to those treated with rhSTC1. Osteoblast subcultures were untreated or were treated with oligonucleotides (3 μM; AS, antisense; SCR, scrambled; INV, inverted) specific to STC1 for 5 days. *, $P < 0.05$, compared with vehicle (−). Semiquantitative RT-PCR reveals the downregulation of Pit1 as well as OPN mRNA. The inset in the right-hand graph shows Western blotting documenting the specific knockdown of STC1 by AS but not two control oligonucleotides. See above for semiquantitative RT-PCR and Western blotting. L32 and actin were used as internal controls in assays shown in panels A to C and D, respectively.

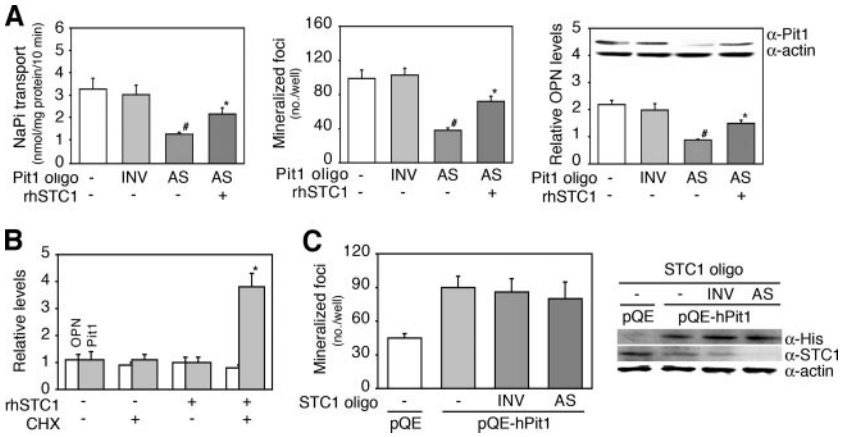

FIG. 5. STC1 is functionally coupled to Pit1 for mineralization in vitro. (A) Coupling of Pit1 and STC1 is involved in mineralization. rhSTC1 partially rescued the decrease in NaP_i transport, mineralization, and OPN mRNA expression elicited by AS knockdown of Pit1 (AS Pit1 oligo). Western blotting (inside the right-hand graph) and semiquantitative RT-PCR reveal that Pit1 protein and OPN mRNA levels were highly synchronized with NaP_i transport activity and mineralization. Osteoblast subcultures were treated with or without 2 μM Pit1 oligonucleotides (Pit1 oligo, AS, or INV) in combination with or without 20 ng/ml rhSTC1 for 5 days. *, $P < 0.05$, and #, $P < 0.05$, compared with AS and vehicle (−), respectively. (B) Superinduction of Pit1 mRNA expression in response to rhSTC1 in the presence of cycloheximide (CHX). Osteoblast subcultures under serum-free conditions were treated with 20 ng/ml rhSTC1 in the presence or absence of 2 μg/ml CHX for 3 h and subjected to semiquantitative RT-PCR analysis. *, $P < 0.01$, compared with vehicle (−). (C) AS knockdown of STC1 had no detectable effect on the increased mineralization seen with hPit1-overexpressing cultures. Osteoblast subcultures were transfected with pQE-hPit1, followed by treatment with STC1 oligonucleotides (3 μM AS or INV) for 6 days. Western blotting shows that overexpression of hPit1 by pQE-hPit1 is not affected by AS knockdown of STC1. L32 and actin were used as internal controls for assays shown in panels B and A and C, respectively.

pQE-hPit1 (Fig. 5C). These data demonstrate an STC1-Pit1 pathway linked to mineralization, in which STC1 stimulates Pit1 mRNA expression, resulting in increased NaP_i transport in mature osteoblast cultures and, vice versa, STC1 expression is regulated by P_i levels in a sensing system in which Pit1 rather than STC1 may be rate limiting.

Finally, we asked whether rhSTC1 alters osteoid mineralization during de novo bone formation in vivo, using the same newborn rat calvaria model described above. The thickness of the osteoid layer in the rhSTC1-treated group was thinner than that in vehicle-injected control animals, but no changes were detectable either in other histomorphometric features (Fig. 6A to C) or in the systemic serum parameters described above (Table 3). In addition, Pit1 and OPN mRNA levels were higher in the calvaria treated with rhSTC1 than those of the controls (Fig. 6D). These in vivo results were entirely consistent with those in the osteoid nodule culture model and suggest that STC1 is a potent regulator of osteoid mineralization.

DISCUSSION

We have shown that NaP_i transport in osteoblasts is indispensable for osteoid mineralization in rapidly growing rat bones. By using the osteoblast subculture model (fully differentiated osteoblast cultures), we have also shown that a carefully regulated level of NaP_i transport via the type III NaP_i transporter Pit1 is required for mineralization independently of effects on cellular proliferation and differentiation. STC1 expression is sensitive to P_i levels and, vice versa, regulates Pit1 expression and thereby NaP_i transport. Thus, our results strengthen the hypothesis that mature osteoblasts control bone mineralization via an endogenous P_i-sensing system (Fig. 7), whose disruption may cause mineralization defects independently of systemic P_i homeostasis.

It has been generally assumed that P_i is required for bone formation, and growing evidence implicates P_i signaling in the induction of OPN, among other genes, and osteoblast differentiation (3, 5), although the underlying mechanisms are still largely unknown (4). Because mineralization defects are seen with increasing osteoid width in autosomal dominant hypophosphatemic rickets (ADHR) (1) and Fgf23-null mice (34, 35) and Hyp mice (18), it is becoming increasingly important to separate the mineralization effects of P_i from cellular proliferation and differentiation effects. To this end, we manipulated the RC cell culture model to separate responses to P_i during osteoblast development from those during the mineralization phase. We combined this with Pit1 and STC1 gain-of-function, loss-of-function, and rescue experiments at specific differentiation stages in vitro and in vivo. By these approaches, we show for the first time the functional role of osteoblast Pit1 in mineralization without its possible confounding effects on osteoblast proliferation and differentiation. Taken together with recent data for MC3T3-E1 cells treated long term with BMP2 (36), the data provide strong support for Pit1-mediated P_i-dependent regulation of bone formation. Indeed, P_i has been shown to regulate multiple genes during MC3T3-E1 osteoblast differentiation, including the transcription factor Nrf2 (4).

Not only our data but also other recent observations such as those with Fgf23-null mice, which exhibit mineralization defects even under hyperphosphatemic conditions (34, 35), underscore the need to determine whether and how locally produced phosphaturic factors act to regulate local P_i homeostasis in bone. For example, loss of DMP1, which is abundant in osteocytes, was found to cause a mineralization defect with elevated FGF23 levels in both human and mouse models (15), providing new insights into osteocyte function and mineral metabolism. Notably, we identified STC1 but not several

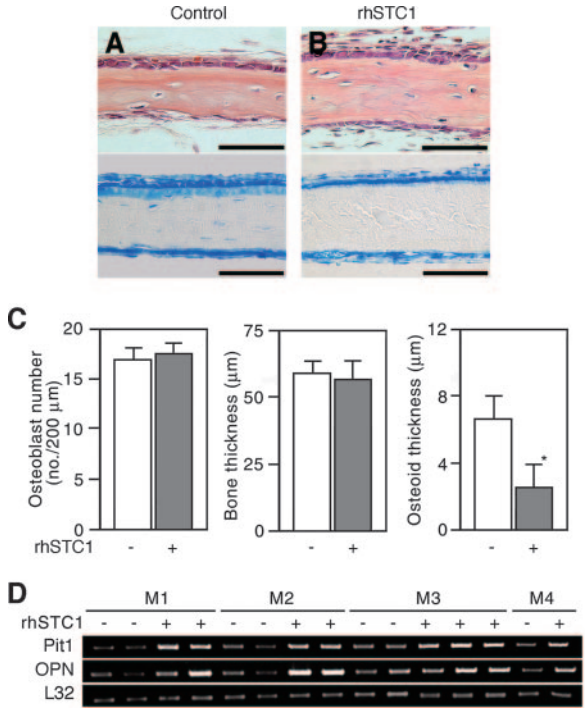

FIG. 6. Bone mineralization progresses rapidly in response to injection of rhSTC1 over the sagittal suture of calvariae of newborn rats. (A and B) Transverse sections of the parietal bone treated with (B) or without (control) (A) rhSTC1 (5 μg/kg/day) for 5 days. Decalcified and paraffin-embedded sections stained with hematoxylin and eosin (upper panels) and plastic sections stained with toluidine blue (lower panels), respectively. Scale bars represent 50 μm. (C) A decrease in osteoid seams without any detectable change in either total bone thickness or osteoblast number in rhSTC1-treated calvariae (closed column). *, $P < 0.05$, compared with vehicle (−). (D) Pit1 and OPN mRNA levels are increased in RNA samples from individual calvaria of animals treated with rhSTC1 (+) compared to those of vehicle-treated animals (−). M*n* indicates individual mothers and their pups; M1 to M3 each had four pups and M4 had two pups treated as indicated. Semiquantitative PCR was used to estimate changes in gene expression (see Materials and Methods); a representative agarose gel is shown. L32 was used as an internal control.

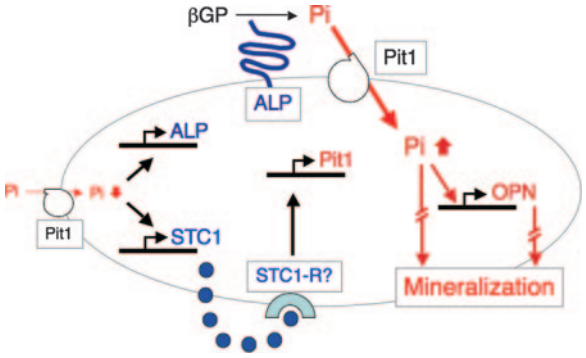

FIG. 7. A schematic of the STC1-Pit1-P_i-sensing system in osteoblasts, deduced from this study. Among all elements that act to enhance bone mineralization, NaP_i transport via Pit1 is a rate-limiting step in mineralization. Low levels of NaP_i transport stimulate STC1 and ALP expression. STC1, as an autocrine/paracrine factor via a putative unknown receptor (perhaps STC1-R), induces Pit1 expression directly to increase NaP_i transport. Increased intracellular P_i increases OPN expression and stimulates mineralization.

known phosphaturic factors, including FGF23 and DMP1, in our screening of candidate early response genes differentially expressed in control versus foscarnet-treated osteoblasts. STC1, similarly to many other osteotropic factors capable of increasing NaP_i transport as described above, not only increases mineralization but also increases osteoblast differentiation in parallel with its NaP_i transport activity (42). Two different TG mouse lines overexpressing STC1 via either a muscle-specific myosin light chain promoter (16) or a metallothionein I promoter (40) have been made. Among the effects observed, growth was retarded with elevated P_i and decreased ALP levels in sera of both models; and bone formation, but not mineralization, was decreased with a suppression of osteoclast activity only in the former TG mouse model (16). In contrast to these two TG mouse lines, Stc1-null mice display no detectable anomalies in growth, reproduction, or a variety of other phenotypic parameters tested (10). The reasons for these discrepancies are currently not known; however, in addition to the complexity of both systemic (see introduction) and skeletal (see below) P_i regulation, the existence of STC1 variants (27) and STC2 (which has 35% sequence identity with STC1) (19 and see below) may play a compensatory and/or an interacting role(s) when STC1 expression is chronically altered. Together with the fact that an STC1-specific receptor has not yet been identified, the data suggest that it may be difficult to detect direct effects on osteoblasts and mineralization from indirect effects in these genetically engineered models. An alternate approach used here was to acutely and locally modify STC1 expression levels at specific developmental times, an approach that is achievable in both our in vivo and in vitro models and that uncovered the functional involvement of STC1 in Pit1-

TABLE 3. Effects of local injections of STC1 over the newborn rat calvaria for 5 days on serum and body weight parameters

STC1 dosage (μg/kg/day)	Effects of STC1 injection (± SD) on the indicated parameters[a]					
	Body wt (g)		Serum concn			
	Day 0	Day 4	Ca (mg/dl)	P_i (mg/dl)	ALP (U/liter)	$1,25(OH)_2D_3$ (pg/ml)
Control	6.16 ± 0.33	13.1 ± 0.41	10.6 ± 0.43	8.9 ± 0.32	233 ± 13	151
2	6.40 ± 0.36	13.3 ± 0.35	10.2 ± 0.33	9.1 ± 0.43	242 ± 19	160
5	6.17 ± 0.38	12.9 ± 0.29	10.7 ± 0.25	9.2 ± 0.44	237 ± 15	149
15	6.24 ± 0.39	13.5 ± 0.45	10.6 ± 0.35	9.1 ± 0.27	240 ± 19	156

[a] Values shown are means ± standard deviations. $1,25(OH)_2D_3$ concentrations were measured in serum pooled from 7 rats per group.

mediated mineralization. Likewise, the administration of recombinant STC1 in vitro or in vivo revealed another biological activity; i.e., STC1 protects neural cells from ischemic challenges with increasing NaP_i transport (43).

Stimulation of NaP_i transport above a critical threshold, e.g., by very high levels of extracellular P_i (over 5 mM [25]), by high overexpression of Pit1 (which, similarly to high P_i levels, causes cell death, see above and Fig. 1G), by hyperphosphatemia, as seen in Fgf23-null mice (34, 35), and possibly by high systemic STC1 levels (16, 40), impacts negatively on osteoblast development. Similarly, we found that exogenous overexpression of hPit1 may culminate in the downregulation of endogenous Pit1. However, smaller increases in NaP_i transport such as those we show here with concomitant smaller changes in intracellular P_i act positively on mineralization and osteoblast-specific signaling, consistent with observations made initially by Bellows et al. (7) and recently by Beck et al. (3). Thus, osteoblast development and activity, including mineralization, function appropriately over a relatively narrow range of NaP_i transport, consistent with Pit1 rather than STC1 being rate limiting in an osteoblast-autonomous Pit1-P_i sensing system for bone mineralization. The manipulation of this autonomous regulatory system, therefore, may offer a novel approach to clarifying the cellular basis of certain skeletal and mineral disorders.

ACKNOWLEDGMENTS

We thank Shoichi Takano and Akira Igarashi of BML (Saitama, Japan) for providing rhSTC1 and anti-rhSTC1 and Takashi Takata of Hiroshima University for providing a human cementing fibroma cell line. We also thank Edith Bonnelye for helpful comments on the manuscript, Dominic Falconi for his helpful discussions, and Usha Bhargava and Tomoko Minamizaki for their technical assistance.

This work was supported by grants-in-aid from the Ministry of Education, Science, Sports and Culture of Japan (13771074 and 16591828 to Y.Y.) and by the Canadian Institutes of Health Research (MT-12390 and MOP-69198 to J.E.A.).

REFERENCES

1. **ADHR Consortium.** 2000. Autosomal dominant hypophosphataemic rickets is associated with mutations in FGF23. Nat. Genet. **26:**345–348.
2. **Aubin, J. E., J. B. Lain, and G. S. Stein.** 2006. Bone formation: maturation and functional activities of osteoblast lineage cells, p. 20–29. *In* M. J. Favus (ed.), Primer on the metabolic bone diseases and disorders of mineral metabolism, 6th ed. American Society for Bone and Mineral Research, Washington, DC.
3. **Beck, G. R., Jr., and N. Knecht.** 2003. Osteopontin regulation by inorganic phosphate is ERK1/2-, protein kinase C-, and proteasome-dependent. J. Biol. Chem. **278:**41921–41929.
4. **Beck, G. R., Jr.** 2003. Inorganic phosphate as a signaling molecule in osteoblast differentiation. J. Cell. Biochem. **90:**234–243.
5. **Beck, G. R., Jr., B. Zerler, and E. Moran.** 2000. Phosphate is a specific signal for induction of osteopontin gene expression. Proc. Natl. Acad. Sci. USA **97:**8352–8357.
6. **Beck, L., A. C. Karaplis, N. Amizuka, A. S. Hewson, H. Ozawa, and H. S. Tenenhouse.** 1998. Targeted inactivation of Npt2 in mice leads to severe renal phosphate wasting, hypercalciuria, and skeletal abnormalities. Proc. Natl. Acad. Sci. USA **95:**5327–5377.
7. **Bellows, C. G., J. N. Heersche, and J. E. Aubin.** 1992. Inorganic phosphate added exogenously or released from β-glycerophosphate initiates mineralization of osteoid nodules in vitro. Bone Miner. **17:**15–29.
8. **Bellows, C. G., J. E. Aubin, J. N. M. Heersche, and M. E. Antosz.** 1986. Mineralized bone nodules formed in vitro from enzymatically released rat calvaria cell populations. Calcif. Tissue Int. **38:**143–154.
9. **Berndt, T., T. A. Craig, A. E. Bowe, J. Vassiliadis, D. Reczek, R. Finnegan, S. M. Jan De Beur, S. C. Schiavi, and R. Kumar.** 2003. Secreted frizzled-related protein 4 is a potent tumor-derived phosphaturic agent. J. Clin. Investig. **112:**785–794.
10. **Chang, A. C., J. Cha, F. Koentgen, and R. R. Reddel.** 2005. The murine stanniocalcin 1 gene is not essential for growth and development. Mol. Cell. Biol. **25:**10604–10610.
11. **Chang, A. C., J. Janosi, M. Hulsbeek, D. de Jong, K. J. Jeffrey, J. R. Noble, and R. R. Reddel.** 1995. A novel human cDNA highly homologous to the fish hormone stanniocalcin. Mol. Cell. Endocrinol. **112:**241–247.
12. **De Beur, S. M., R. B. Finnegan, J. Vassiliadis, B. Cook, D. Barberio, S. Estes, P. Manavalan, J. Petroziello, S. L. Madden, J. Y. Cho, R. Kumar, M. A. Levine, and S. C. Schiavi.** 2002. Tumors associated with oncogenic osteomalacia express genes important in bone and mineral metabolism. J. Bone Miner. Res. **17:**1102–1110.
13. **Ecarot, B., F. H. Glorieux, M. Desbarats, R. Travers, and L. L. Labelle.** 1992. Defective bone formation by Hyp mouse bone cells transplanted into normal mice: evidence in favor of an intrinsic osteoblast defect. J. Bone Miner. Res. **7:**215–220.
14. **Edwards, D. R., and L. C. Mahadevan.** 1992. Protein synthesis inhibitors differentially superinduce c-fos and c-jun by three distinct mechanisms: lack of evidence for labile repressors. EMBO J. **11:**2415–2424.
15. **Feng, J. Q., L. M. Ward, S. Liu, Y. Lu, Y. Xie, B. Yuan, X. Yu, F. Rauch, S. I. Davis, S. Zhang, H. Rios, M. K. Drezner, L. D. Quarles, L. F. Bonewald, and K. E. White.** 2006. Loss of DMP1 causes rickets and osteomalacia and identifies a role for osteocytes in mineral metabolism. Nat. Genet. **38:**1310–1315.
16. **Filvaroff, E. H., S. Guillet, C. Zlot, M. Bao, G. Ingle, H. Steinmetz, J. Hoeffel, S. Bunting, J. Ross, R. A. Carano, L. Powell-Braxton, G. F. Wagner, R. Eckert, M. E. Gerritsen, and D. M. French.** 2002. Stanniocalcin 1 alters muscle and bone structure and function in transgenic mice. Endocrinology **143:**3681–3690.
17. **Hisano, S., H. Haga, Z. Li, S. Tatsumi, K. I. Miyamoto, E. Takeda, and Y. Fukui.** 1997. Immunohistochemical and RT-PCR detection of Na+-dependent inorganic phosphate cotransporter (NaPi-2) in rat brain. Brain Res. **772:**149–155.
18. **HYP Consortium.** 1995. A gene (PEX) with homologies to endopeptidases is mutated in patients with X-linked hypophosphatemic rickets. Nat. Genet. **11:**130–136.
19. **Ishibashi, K., K. Miyamoto, Y. Taketani, K. Morita, E. Takeda, S. Sasaki, and M. Imai.** 1998. Molecular cloning of a second human stanniocalcin homologue (STC2). Biochem. Biophys. Res. Commun. **250:**252–258.
20. **Karsenty, G., and E. F. Wagner.** 2002. Reaching a genetic and molecular understanding of skeletal development. Dev. Cell **2:**389–406.
21. **Kavanaugh, M. P., D. G. Miller, W. Zhang, W. Law, S. L. Kozak, D. Kabat, and A. D. Miller.** 1994. Cell-surface receptors for gibbon ape leukemia virus and amphotropic murine retrovirus are inducible sodium-dependent phosphate symporters. Proc. Natl. Acad. Sci. USA **91:**7071–7075.
22. **Kimmel, C. A., and C. Trammell.** 1981. A rapid procedure for routine double staining cartilage and bone in fetal and adult animals. Stain Technol. **56:** 271–273.
23. **Larsson, T., R. Marsell, E. Schipani, C. Ohlsson, O. Ljunggren, H. S. Tenenhouse, H. Juppner, and K. B. Jonsson.** 2004. Transgenic mice expressing fibroblast growth factor 23 under the control of the α1 (I) collagen promoter exhibit growth retardation, osteomalacia, and disturbed phosphate homeostasis. Endocrinology **145:**3087–3094.
24. **Li, X., H. Y. Yang, and C. M. Giachelli.** 2006. Role of the sodium-dependent phosphate cotransporter, Pit-1, in vascular smooth muscle cell calcification. Circ. Res. **98:**905–912.
25. **Meleti, Z., I. M. Shapiro, and C. S. Adams.** 2000. Inorganic phosphate induces apoptosis of osteoblast-like cells in culture. Bone **27:**359–366.
26. **Mundy, G., R. Garrett, S. Harris, S. J. Chan, D. Chen, G. Rossini, B. Boyce, M. Zhao, and G. Gutierrez.** 1999. Stimulation of bone formation in vitro and in rodents by statins. Science **286:**1946–1949.
27. **Paciga, M., C. R. McCudden, C. Londos, G. E. DiMattia, and G. F. Wagner.** 2003. Targeting big stanniocalcin and its receptor to lipid storage droplets of ovarian steroidogenic cells. J. Biol. Chem. **278:**49549–49554.
28. **Palmer, G., J. Guicheux, J. P. Bonjour, and J. Caverzasio.** 2000. Transforming growth factor-β stimulates inorganic phosphate transport and expression of the type III phosphate transporter Glvr-1 in chondrogenic ATDC5 cells. Endocrinology **141:**2236–2243.
29. **Palmer, G., J. P. Bonjour, and J. Caverzasio.** 1997. Expression of a newly identified phosphate transporter/retrovirus receptor in human SaOS-2 osteoblast-like cells and its regulation by insulin-like growth factor I. Endocrinology **138:**5202–5209.
30. **Pizurki, L., R. Rizzoli, J. Caverzasio, and J. P. Bonjour.** 1991. Stimulation by parathyroid hormone-related protein and transforming growth factor-α of phosphate transport in osteoblast-like cells. J. Bone Miner. Res. **6:**1235–1241.
31. **Quarles, L. D.** 2003. Evidence for a bone-kidney axis regulating phosphate homeostasis. J. Clin. Investig. **112:**642–646.
32. **Rowe, P. S. N., P. de Zoysa, R. Dong, H. Wang, K. White, M. J. Econs, and C. L. Oudet.** 2000. MEPE, a new gene expressed in bone-marrow and tumors causing osteomalacia. Genomics **67:**54–68.
33. **Sato, T., T. Maekawa, S. Watanabe, K. Tsuji, and T. Nakahata.** 2000. Erythroid progenitors differentiate and mature in response to endogenous erythropoietin. J. Clin. Investig. **16:**263–270.
34. **Shimada, T., M. Kakitani, Y. Yamazaki, H. Hasegawa, Y. Takeuchi, T. Fujita, S. Fukumoto, K. Tomizuka, and T. Yamashita.** 2004. Targeted abla-

tion of Fgf23 demonstrates an essential physiological role of FGF23 in phosphate and vitamin D metabolism. J. Clin. Investig. **113:**561–568.
35. **Sitara, D., M. S. Razzaque, M. Hesse, S. Yoganathan, T. Taguchi, R. G. Erben, H. Juppner, and B. Lanske.** 2004. Homozygous ablation of fibroblast growth factor-23 results in hyperphosphatemia and impaired skeletogenesis and reverses ypophosphatemia in Phex-deficent mice. Matrix Biol. **23:**421–432.
36. **Suzuki, A., C. Ghayor, J. Guicheux, D. Magne, S. Quillard, A. Kakita, Y. Ono, Y. Miura, Y. Oiso, M. Itoh, and J. Caverzasio.** 2006. Enhanced expression of the inorganic phosphate transporter Pit-1 is involved in BMP-2-induced matrix mineralization in osteoblast-like cells. J. Bone Miner. Res. **21:**674–683.
37. **Suzuki, A., G. Palmer, J. P. Bonjour, and J. Caverzasio.** 2000. Stimulation of sodium-dependent phosphate transport and signaling mechanisms induced by basic fibroblast growth factor in MC3T3-E1 osteoblast-like cells. J. Bone Miner. Res. **15:**95–102.
38. **Swenson, C. L., S. E. Weisbrode, L. A. Nagode, K. A. Hayse, C. L. Steinmeyer, and L. E. Mathes.** 1991. Age-related differences in phosphonoformate-induced bone toxicity in cats. Calcif. Tissue Int. **48:**353–361.
39. **Tenenhouse, H. S., C. Gauthier, J. Martel, F. A. Gesek, B. A. Coutermarsh, and P. A. Friedman.** 1998. Na^+-phosphate cotransport in mouse distal convoluted tubule cells: evidence for Glvr-1 and Ram-1 gene expression. J. Bone Miner. Res. **13:**590–597.
40. **Varghese, R., A. D. Gagliardi, P. E. Bialek, S. P. Yee, G. F. Wagner, and G. E. Dimattia.** 2002. Overexpression of human stanniocalin affects growth and reproduction in transgenic mice. Endocrinology **143:**868–876.
41. **Wennberg, C., L. Hessle, P. Lundberg, S. Mauro, S. Narisawa, U. H. Lerner, and J. L. Millan.** 2000. Functional characterization of osteoblasts and osteoclasts from alkaline phosphatase knockout mice. J. Bone Miner. Res. **15:**1879–1888.
42. **Yoshiko, Y., N. Maeda, and J. E. Aubin.** 2003. Stanniocalcin 1 stimulates osteoblast differentiation in rat calvaria cell cultures. Endocrinology **144:**4134–4143.
43. **Zhang, K., P. J. Lindsberg, T. Tatlisumak, M. Kaste, H. S. Olsen, and L. C. Andersson.** 2000. Stanniocalcin: a molecular guard of neurons during cerebral ischemia. Proc. Natl. Acad. Sci. USA **97:**3637–3642.
44. **Zhen, X., J. P. Bonjour, and J. Caverzasio.** 1997. Platelet-derived growth factor stimulates sodium-dependent Pi transport in osteoblastic cells via phospholipase Cγ and phosphatidylinositol 3′-kinase. J. Bone Miner. Res. **12:**36–44.